Synthesis and Characterization of a Novel Hybrid Material Titanium Amino Tris(methylenephosphonic acid) and Its Application as a Cation Exchanger

ARTICLE *in* INDUSTRIAL & ENGINEERING CHEMISTRY RESEARCH · OCTOBER 2014

Impact Factor: 2.59 · DOI: 10.1021/ie502673m

2 AUTHORS:

Brijesh Shah
The Maharaja Sayajirao University of Baroda
6 PUBLICATIONS **15** CITATIONS
SEE PROFILE

Uma Chudasama
The Maharaja Sayajirao University of Baroda
81 PUBLICATIONS **456** CITATIONS
SEE PROFILE

I&EC research
Industrial & Engineering Chemistry Research

Article

pubs.acs.org/IECR

Synthesis and Characterization of a Novel Hybrid Material Titanium Amino Tris(methylenephosphonic acid) and Its Application as a Cation Exchanger

Brijesh Shah and Uma Chudasama*

Applied Chemistry Department, Faculty of Technology & Engineering, The M. S. University of Baroda, Post Box No. 51, Kalabhavan, Vadodara 390 001, Gujarat, India

Supporting Information

ABSTRACT: In the present work, a novel hybrid ion-exchange material was synthesized by a sol−gel route, by treating titanium tetrachloride with claw-type amino tris(methylenephosphonic acid) (ATMP) to give titanium amino tris(methylenephosphonic acid) (Ti-ATMP). Ti-ATMP was characterized by elemental analysis (ICP-AES and C, H, N analysis), spectral analysis (FTIR), thermal analysis (TGA), XRD, SEM, and EDX spectroscopy, including physicochemical and ion-exchange characteristics. The equilibrium exchange of transition-metal ions (viz., Cu^{2+}, Ni^{2+}, Co^{2+} Zn^{2+}) and heavy-metal ions (viz., Pb^{2+},Cd^{2+}, Hg^{2+}) with the H^+ ions contained in ATMP was studied at constant ionic strength and varying temperatures, and various thermodynamic parameters such as the equilibrium constant (K), standard Gibbs free energy (ΔG°), enthalpy (ΔH°), and entropy (ΔS°) were evaluated. The Nernst−Planck equation was used to study the ion-exchange kinetics, and various kinetic parameters, namely, the self-diffusion coefficient (D_0), energy of activation (E_a), and entropy of activation (ΔS^*), were evaluated under conditions favoring a particle-diffusion-controlled mechanism. Metal-ion adsorptions with variations in concentration and temperature were studied using the Langmuir and Freundlich adsorption isotherms. The distribution coefficient (K_d) and breakthrough capacity (BTC) values for transition- and heavy-metal ions were determined. Based on K_d ($mL \cdot g^{-1}$), the selectivity order for metal ions toward Ti-ATMP was found to be Cu^{2+} (19820) > Zn^{2+}(3280) > Co^{2+} (2630) > Ni^{2+} (2390) among transition-metal ions and Pb^{2+} (3590) > Cd^{2+} (2340) > Hg^{2+} (610) among the heavy-metal ions. The elution behavior of these metal ions was studied using different acids and electrolytes. A study on regeneration and reuse of the ion exchanger Ti-ATMP shows that it is effective up to five cycles without much decline in performance, which indicates that Ti-ATMP has good potential for use as a cation exchanger.

1. INTRODUCTION

Development of sensitive and mature technologies for the removal of heavy-metal ions from aqueous solutions has been an important scientific endeavor during the past few years. Several separation methods such as precipitation, membrane processes, adsorption based on activated carbons, solid phase extraction, and use of chelating exchangers[1−4] are available for the removal of heavy-metal ions from aqueous solutions. Further, an extensive literature is also available on modifying the surface of silica with organic-based absorbent materials utilized for the removal of lead,[2,5,6] copper,[6] mercury,[6] and cadmium,[6−8]

Among various processes developed to remove metal ions from wastewater, it has been observed that, at low concentrations, the removal is more effective by ion exchange.[9,10] There has been substantial research on both inorganic ion exchangers[11,12] and organic resins for the remediation of wastewater containing toxic metals.[11,12] Because both exchangers have limitations, research has been motivated to study inorganic−organic hybrid ion exchangers[12] that could offer better composite properties in terms of chemical, mechanical, and thermal stabilities and good selectivity for metal ions.[12,13] Further, inorganic−organic hybrids based on the functionalization or modification of organosilicas is confined to the physical properties concerned with adsorption, ion exchange, and catalysis, and thereby, the rational design of hybrid materials has been extended to nonsiliceous organic−inorganic hybrid materials including metal phosphonates.[14]

A major advantage of inorganic−organic hybrid materials is the rigid inorganic backbone and the flexibility of the organic groups, which provide a wide range of properties.[15] Anchoring of organic units on the backbone of tetravalent metal acid (TMA) salts is of particular interest. Synthesis of inorganic ion exchangers in the class of TMA salts has been an area of considerable study owing to the high selectivity of these materials for certain metal ions and excellent ion-exchange behavior.[9,16,17] TMA salts are cation exchangers that exhibit the general formula $M^{IV}(HXO_4)_2 \cdot nH_2O$, where M^{IV} = Zr, Ti, Sn, Ce, Th, and X = P, Mo, W, As, Sb, and so on. They contain structural hydroxyl protons, the H^+ ions of the —OH groups being the exchangeable sites. A number of cations can be exchanged with H^+, as a result of which TMA salts exhibit cation-exchange properties.[9,17,18] M(IV) phosphates of the class of TMA salts were previously proposed for use as ion exchangers.[17−20] These phosphates have also shown a number of advantages as an ideal host lattice.[21] In the tetrahedral moiety of phosphoric acid, $PO(OH)_3$, if H or OH is replaced

Received: July 9, 2014
Revised: October 2, 2014
Accepted: October 14, 2014
Published: October 14, 2014

dx.doi.org/10.1021/ie502673m | Ind. Eng. Chem. Res. 2014, 53, 17454−17467

by R (where R is an alkyl/aryl moiety containing ionogenic groups such as —COOH, —OH, and —SO_3H), phosphonic acids are obtained, which, when treated, with tetravalent metals such as Zr, Ti, Sn, Th, Ce, and so on give rise to novel metal phosphonates. Much interest has been generated in the field of metal phosphonates in the past decade,[22−26] where the focus has been on synthesis and structural elucidation. In these publications,[22−28] the possible use of metal phosphonates as ion exchangers, proton conductors, adsorbents, and catalysts has been proposed. M(IV) phosphonates [where M(IV) = Zr or Ti and phosphonic acid = HEDP (hydroxyethylidene diphosphonic acid)] has been synthesized, and its application in heavy-metal-ion adsorption[13,29−31] as well as ion exchangers for metal separation has been explored.[32,33]

Aminophosphonic acids contain donor groups that are effective in the binding of tetravalent metal ions, and so, these acids have received considerable attention because of their diverse binding abilities.[34,35] A porous titanium phosphonate, titanium amino tris(methylenephosphonic acid), has been synthesized by a hydrothermal process[36] and used for the adsorption of heavy-metal ions. Further, hollow manganese phosphonate prepared by a templet-free hydrothermal method was utilized in the removal of Cu^{2+} metal ion.[37] Our laboratory has reported the synthesis, using diethylenetriamine pentakis-(methylenephosphonic acid), of zirconium-[38] and titanium-based[39] phosphonates that exhibit cation-exchange capacities (CECs) of 2.34 and 3.56 mequiv/g, respectively. These materials have been used as cation exchangers for metal-ion separations.[38,39] Zirconium amino tris(methylene phosphonic acid) (Zr-ATMP) with a CEC of 3.61 mequiv/g was synthesized and characterized by us earlier, and its possible use as a cation exchanger was explored.[40]

In the present work, an amorphous titanium amino tris(methylene phosphonic acid) (Ti-ATMP) with an appreciable CEC value was synthesized by a sol−gel route. ATMP (Figure 1) containing six structural hydroxyl groups, compared

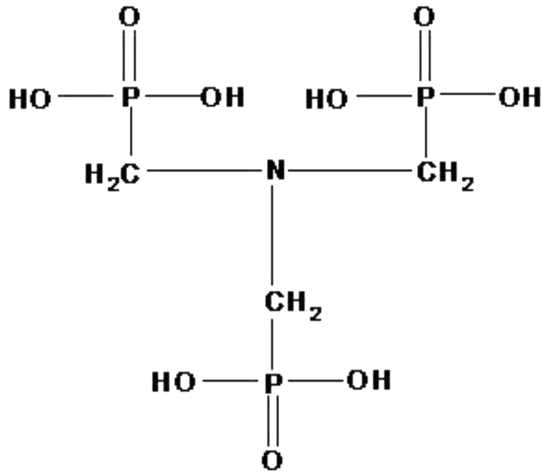

Figure 1. Structure of ATMP.

to phosphoric acid (H_3PO_4), which contains three structural hydroxyl groups, was used with the intention of obtaining higher a cation-exchange capacity in terms of pendant hydroxyl groups in the resulting metal phosphonate. The material was characterized by elemental analysis [inductively coupled plasma atomic emission spectroscopy (ICP-AES) and C, H, N analysis], spectral analysis [Fourier transform infrared (FTIR) spectroscopy], thermal analysis [thermogravimetric analysis (TGA)], X-ray diffraction (XRD), scanning electron microscopy (SEM), and energy-dispersive X-ray (EDX) spectroscopy. The physical and ion-exchange characteristics of the material, as well as its chemical stability in various acids, bases, and organic solvent media, were assessed. The equilibrium exchange of transition-metal ions (Cu^{2+}, Ni^{2+}, Co^{2+}, Zn^{2+}) and heavy-metal ions (Pb^{2+}, Cd^{2+}, Hg^{2+}) with the H^+ ions contained in ATMP was studied at varying temperatures and constant ionic strength, and various thermodynamic parameters such as the equilibrium constant (K), standard Gibbs free energy (ΔG°), enthalpy (ΔH°), and entropy (ΔS°) were evaluated. The Nernst−Planck equation was used to study the ion-exchange kinetics, and various kinetic parameters including the self-diffusion coefficient (D_0), energy of activation (E_a), and entropy of activation (ΔS^*) were evaluated under conditions favoring a particle-diffusion-controlled mechanism. Variations in metal-ion adsorption with concentration and temperature were studied by the Langmuir and Freundlich adsorption isotherms. The distribution coefficient (K_d) and breakthrough capacity (BTC) for metal ions under study were determined. The elution behaviors of these metal ions were studied using acids and electrolytes. Based on the separation factor α, a few binary and ternary metal-ion separations were carried out.

2. EXPERIMENTAL SECTION

Titanium tetrachloride ($TiCl_4$) was procured from Loba Chemicals. Amino tris(methylene phosphonic acid) (ATMP; 50%, ∼1.18 M) with a density of 1.3 g/cm^2 and a molecular weight of 299.04 g (CAS No. 6419-19-8) was obtained from Hydrochem India Pvt. Ltd. The appropriate/required concentration of ATMP was prepared from 50% (∼1.18 M) ATMP solution for the synthesis of Ti-ATMP. All chemicals and reagents used were of analytical grade. Deionized water (DIW) was used in all of the studies.

2.1. Synthesis of Ti-ATMP. The main objective of the synthesis was to prepare a material with a maximum cation-exchange capacity (CEC) that is highly insoluble and chemically resistant to any media in which an exchanger would be used.

2.1.1. Synthesis of Ti-ATMP under Optimized Conditions. Ti-ATMP was prepared by mixing aqueous solutions of ATMP (0.2 M, 50 mL) and $TiCl_4$ (0.1 M, 50 mL in 10% H_2SO_4 solution) at room temperature, dropwise and with continuous stirring. A gelatinous precipitate was obtained, and the solution along with the precipitate was further stirred for 1 h. The resulting gelatinous precipitate was allowed to stand for 3 h and then filtered, washed with DIW until the removal of the chloride ions, and then dried at room temperature. The material was then broken down to the desired particle size of 30−60 mesh (ASTM) by grinding and sieving and converted to the acid form by taking 5 g of the material and treating it with 50 mL of 1 M HNO_3 for 30 min with occasional shaking. The material was then separated from the acid by decantation and washed with DIW to remove the adhering acid. This process (acid treatment) was repeated at least five times. After the final washing, the material was dried at room temperature. This material was used for all studies (Supporting Information, Table S1).

2.2. Physicochemical and Ion-Exchange Characterization. Physical characteristics such as appearance, percentage moisture content, apparent density, and true density and ion-exchange characteristics such as void volume fraction,

concentration of fixed ionogenic groups, and volume capacity for Ti-ATMP were studied according to known methods.[41−43]

2.2.1. Chemical Resistivity. The chemical stability of Ti-ATMP in various media, namely, acids (HCl, H_2SO_4, and HNO_3), bases (NaOH and KOH), and organic solvents (ethanol, benzene, acetone, and acetic acid), was studied by taking 0.5 g of Ti-ATMP in 50 mL of the particular medium and allowing the mixture to stand for 24 h. Any changes in color, nature, weight, solubility, metal washout, particle size, and so on were observed. To confirm the solubility of the exchanger in a particular medium, the supernatant liquid was checked qualitatively for the respective elements of the exchanger.

2.2.2. pH Titration Curve. In the present case, 500 mg of Ti-ATMP was placed in 100 mL of 0.1 M NaCl solution. This mixture was titrated against NaOH (0.1 M) solution. After addition of every 0.5 mL of titrant, sufficient time was provided for the establishment of equilibrium, until the pH remained constant. A pH titration curve was obtained by plotting pH versus volume of NaOH added[30] (Figure 2).

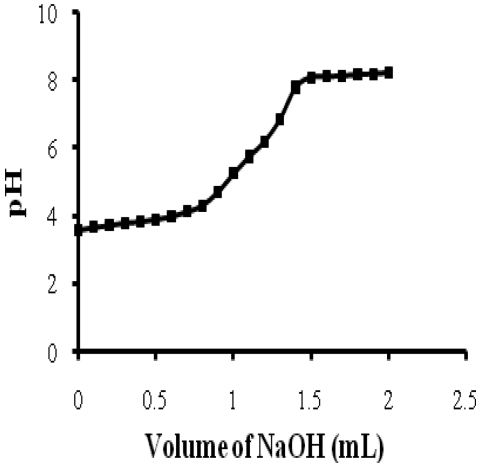

Figure 2. pH titration curve of Ti-ATMP.

2.2.3. Cation-Exchange Capacity (CEC) and Effect of Calcination on CEC. The Na^+ cation-exchange capacity (CEC) of Ti-ATMP was determined by the column method by optimizing the volume and concentration of sodium acetate solution.[38] In the first case, a fixed volume (250 mL) of sodium acetate solution of varying concentration (0.1, 0.2, 0.3, 0.4, 0.5, 0.6, and 0.7 M) was passed through a glass column [30 cm × 1 cm (internal diameter)] containing 0.5 g of the exchanger at a constant flow rate of 0.5 mL·min^{-1}. The effluent (containing eluted H^+ ions) was titrated against 0.1 M NaOH solution. The optimum concentration of eluant was thus determined. In the second case, an eluant of optimum concentration was used, and 10 mL fractions were passed through the column at a constant flow rate of 0.5 mL min^{-1}. This experiment was conducted to determine the minimum volume necessary for the complete elution of H^+ ions, which reflects the efficiency of the column. Using these optimized parameters, the Na^+ CEC was determined as aV/W, where a and V are the molarity and amount of alkali used during the titration, respectively, and W is the weight of the exchanger.

The effect of calcination on the CEC was studied by calcining several 1 g portions of the material for 2 h in the temperature range of 100−500 °C at 100 °C intervals in a muffle furnace, cooling them to room temperature, and determining the CEC by the column method as described above.

2.3. Instrumentation. Ti-ATMP was analyzed for titanium and phosphorus by ICP-AES. FTIR spectra were recorded using the KBr pellet method on a Shimadzu FTIR-8400S spectrometer. Thermogravimetric analysis (TGA) was performed on a Shimadzu TGA-50 thermal analyzer at a heating rate of 10 °C·min^{-1}. X-ray diffractograms (2θ = 10−80°) were obtained on a Bruker AXS D8 X-ray diffractometer with nickel-filtered Cu K_α radiation. SEM and EDX analyses were performed on a JEOL JSM-5610-SLV scanning electron microscope. For thermodynamic and kinetic studies, an electric, temperature-controlled shaker bath having a temperature variation of ±0.5 °C was used.

2.4. Thermodynamic Studies. *2.4.1. Equilibrium Time Determination.* The equilibrium time was determined for Cu^{2+}, and the results obtained were utilized for the other metal ions under study. In these experiments, 0.1 g of exchanger Ti-ATMP (in H^+ form) was shaken with 0.002 M metal-ion solution in a stoppered conical flask for times varying from 30 min to 6 h, in 30-min intervals at a particular temperature (303 K). After each prescribed time interval, the mixture was filtered, and the residual metal-ion concentration in the filtrate was analyzed by titration with ethylenediaminetetraacetic acid (EDTA). The amount of metal ion exchanged was determined from the concentration difference measured between the filtrate and the initial metal-ion solution. A plot of the fractional attainment of equilibrium versus time (t) was used to determine the maximum equilibrium time.

2.4.2. Equilibrium Experiments. Equilibrium experiments were performed by shaking 0.1 g of exchanger particles at the desired temperature (303−333 K in 10 K intervals) in a shaker bath for the optimum equilibrium time of 6 h with 20 mL of a mixture of solution containing 0.06 M HCl and the appropriate metal ion at varying volume ratios (1, 3, 5, ..., and 19 mL of 0.02 M metal-ion solution with 19, 17, 15, ..., and 1 mL, respectively, of 0.06 M HCl) having constant ionic strength (0.06 M). After each prescribed time interval, the metal-ion concentration was determined by EDTA titration as discussed earlier. From these experiments, thermodynamic parameters consisting of the equilibrium constant (K), standard Gibbs free energy change ($\Delta G°$), enthalpy change ($\Delta H°$), and entropy change ($\Delta S°$) were determined.

2.5. Kinetic Studies. *2.5.1. Varying Metal-Ion Concentration.* The effect of concentration on the mechanism of exchange was studied by taking metal-ion solutions of different concentrations (varied from 0.002 to 0.02 M in intervals of 0.002 M) for the ion-exchange process. A 20 mL sample of metal-ion solution at each concentration was shaken with 0.2 g of exchanger (in H^+ form) in a stoppered conical flask at 303 K for different time intervals (0.5, 1.0, 2.0, 3.0, and 4.0 min). After each prescribed time interval, the metal-ion concentration was evaluated by EDTA titration.

2.5.2. Varying Reaction Temperature. For these experiments, Twenty 20 mL of 0.02 M metal-ion solution was shaken with 0.2 g of exchanger in a stoppered conical flask at the desired temperature (303, 313, 323, and 333 K) for different time intervals (0.5, 1.0, 2.0, 3.0, and 4.0 min). After each prescribed time interval, the metal-ion concentration was evaluated by EDTA titration.

2.6. Adsorption Studies. *2.6.1. Effects of pH, Contact Time, and Temperature on Adsorption/Ion Exchange.*

Adsorption/ion exchange of transition-metal ions Co^{2+}, Ni^{2+}, Cu^{2+}, and Zn^{2+} and heavy-metal ions Cd^{2+}, Hg^{2+}, and Pb^{2+} using Ti-ATMP was studied in the pH range of 1−7 by the batch method. In these experiments, 10 mL of 0.002 M metal-ion solution was added to 0.1 g of the exchanger Ti-ATM, the pH was adjusted (using HNO_3 and NaOH in the acidic and alkaline ranges, respectively), and the mixture was shaken for 30 min, after which the metal-ion concentration was determined by EDTA titration. The percentage uptake was calculated as $[(C_0 - C_e)/C_0] \times 100$, where C_0 is the initial concentration of metal ion in mg/L and C_e is the final concentration of metal ion in g/L. A 10 mL sample of 0.02 M metal-ion solution was equilibrated in a stoppered conical flask at the desired temperature (303−333 K in 10 K intervals) for specific time intervals in increments of 10 min (10−200 min). In each case, the pH of the solution was adjusted to the value at which the maximum sorption of the respective metal ion occurs, using 0.1 g of ion exchanger. After each prescribed time interval, the metal-ion concentration was evaluated by EDTA titration.[44]

2.7. Distribution Study and Breakthrough Capacity (BTC). The effects of metal-ion concentration on the distribution coefficient (K_d) for transition-metal ions Co^{2+}, Ni^{2+}, Cu^{2+}, and Zn^{2+} and heavy-metal ions Cd^{2+}, Hg^{2+}, and Pb^{2+} were determined by the batch method. In these experiemnts, 0.1 g of Ti-ATMP in H^+ form was equilibrated with 20 mL of metal-ion solution of varying concentration (0.002−0.02 M in intervals of 0.002 M) for 6 h (maximum equilibrium time) at room temperature. The metal-ion concentrations before and after exchange were determined by EDTA titration.

K_d was also evaluated under the optimum conditions (optimum metal-ion concentration, pH of maximum adsorption, and maximum equilibrium time) using 0.1 g of the exchanger in both water and electrolyte media (0.02 and 0.2 M) such as NH_4NO_3, HNO_3, $HClO_4$, and CH_3COOH at room temperature. K_d was evaluated using the expression $K_d = [(I - F)/F](V/W)$ ($mL \cdot g^{-1}$), where I is the total amount of metal ion in the solution initially, F is the total amount of metal ions left in the solution at equilibrium, V is the volume of the metal-ion solution, and W is the weight of the exchanger in grams.

2.8. Column Preparation. For the BTC determinations, elution studies, and separation studies, the column was prepared as follows: A dry glass column (30 cm length × 1 cm internal diameter) was filled with glass wool at the bottom (height ≈ 1 cm) and washed thoroughly with DIW. Then, 0.5 g of the ion exchanger Ti-ATMP was introduced into the column (bed height = 1.3 cm), followed by glass wool (height ≈ 1 cm) at the top, and the column was washed thoroughly with DIW to remove air bubbles. The flow rate was adjusted to 0.5 $mL \cdot min^{-1}$ for all studies.

2.9. Breakthrough Capacity (BTC). For the determination of the BTC, 0.5 g of the ion exchanger Ti-ATMP was taken in a glass column (as prepared above) and washed thoroughly with DIW, and the flow rate was adjusted to 0.5 $mL \cdot min^{-1}$. Then, 5 mL fractions of each individual metal ion (transition-metal ions Co^{2+}, Ni^{2+}, Cu^{2+}, and Zn^{2+} and heavy-metal ions Pb^{2+}, Cd^{2+}, and Hg^{2+}) at a concentration of 0.002 M was passed through the column, and the effluent was collected until the metal-ion concentrations in the feed and effluent were the same. The breakthrough curve was obtained by plotting the ratio C_e/C_0 against the effluent volume, where C_0 and C_e are the concentrations of the initial solution and the effluent, respectively. BTC was calculated as $(C_0 V_{10\%})/W$ ($mmol \cdot g^{-1}$), where C_0 is the metal-ion initial concentration ($mol \cdot L^{-1}$), $V_{10\%}$ is the volume (mL) of metal-ion solution that had passed through the column when the exit concentration reached 10% of the initial concentration, and W is the weight (mg) of exchanger.

2.10. Elution and Separation Studies. For (single-metal) elution studies, the column was prepared as discussed earlier. The metal-ion solution (0.001 M, 10 mL) was loaded onto the column. The loaded metal ion was eluted with reagents such as HNO_3, $HClO_4$, CH_3COOH, and NH_4NO_3 at concentrations of 0.02 and 0.2 M. The amount of metal ion recovered was calculated in terms of percentage elution, expressed as E (%) = $(C_e/C_0) \times 100$, where C_e is the concentration of metal ion in the eluted solution and C_0 is the concentration of metal ion loaded onto the column.

For binary or ternary separations, the mixture of metal ions (0.001 M, 10 mL for each metal ion) to be separated was loaded onto the column. Metal separations were achieved by passing suitable eluants through the column. For a given metal-ion pair, the eluant was selected based on the K_d values of the respective metal ions (in a particular medium) in which the separation factor was highest. Metal-ion concentrations were determined quantitatively by EDTA titration. For each experimental point in the graphs reported in this article, two identical runs were performed to compare/verify the obtained values. The reproducibility of the value for the same experimental point was assessed by again performing two identical runs. The amount of each metal ion eluted (E, %) was calculated using the same equation as for the single-metal studies.

2.11. Regeneration and Reusability of the Ion Exchanger. The regeneration and reuse of the ion exchanger Ti-ATMP were investigated in the case of copper ion by the batch method. In this case, a Cu^{2+} solution of the optimum concentration (0.014 M) was treated with 0.1 g of Ti-ATMP for 6 h (maximum equilibrium time), after which the metal-ion concentration was determined by EDTA titration and the K_d value determined. The Cu^{2+}-exchanged Ti-ATMP was treated with HNO_3 (1 M, 50 mL) for 30 min with occasional shaking. The Ti-ATMP sample was then separated from the acid by decantation and treated with DIW to remove adhering acid. This process was repeated at least five times to ensure complete removal of Cu^{2+} from the exchanger. This regenerated Ti-ATMP was used to determine K_d values. This process was repeated until wide variations in K_d values were observed. The percentage retention of K_d value, $K_{d(R)}$, was determined in each subsequent cycle using the expression $K_{d(R)} = [K_{d(C)}/K_d] \times 100$, where K_d is the initial value obtained and $K_{d(C)}$ is the value determined in that cycle.

3. RESULTS AND DISCUSSION

3.1. Characterization of Ti-ATMP. The physical and ion-exchange characteristics of Ti-ATMP are presented in Table 1. Ti-ATMP was obtained as hard, pale yellow granules. The elemental analysis of Ti-ATMP, performed by ICP-AES, gave Ti and P contents of 13.01 and 21.12 wt %, respectively. CHN analysis gave the following contents: C, 7.89 wt %; H, 4.54 wt %; and N, 2.99 wt %. These results were well supported by EDX spectroscopy (Figure 3A), which gave Ti and P contents of 13.62 and 20.50 wt %, respectively. The weight percentages of elements found by the instrumental methods of analysis matched well with the theoretical values. Based on the ICP-AES and CHN data, Ti-ATMP was determined to have the formula $Ti(C_3H_{12}NP_3O_9)_{0.9} \cdot 2H_2O$ based on earlier studies on metal

dx.doi.org/10.1021/ie502673m | Ind. Eng. Chem. Res. 2014, 53, 17454−17467

Table 1. Physical and Ion-Exchange Characteristics of Ti-ATMP

characteristic	observation
appearance	hard, pale yellow granules
particle size (μm)	250−590
moisture content (%)	11.52
true density (g·mL^{-1})	1.80
apparent density (g·mL^{-1})	0.27
void volume fraction	0.70
concentration of fixed ionogenic groups (mmol·g^{-1})	1.05
volume capacity of resin (mequiv·mL^{-1})	0.29
nature of exchanger	weak cation exchanger
CEC (mequiv·g^{-1})	
room temperature	4.01
100 °C	3.93
200 °C	3.22
300 °C	3.07
400 °C	2.26
500 °C	1.13
chemical stability (maximum tolerable limits)	
acids	18 N H_2SO_4, 16.3 N HNO_3, 11.3 N HCl
bases	0.02 N NaOH, 0.02 N KOH
organic solvents	ethanol, benzene, acetone, acetic acid

phosphonates.[13,29,39] The Na^+ cation-exchange capacity (CEC) evaluated by the column method at room temperature was 4.01 mequiv·g^{-1} (Supporting Information, Figures S1 and S2), indicating that the minimum molar concentration and optimum volume of sodium acetate solution for maximum elution of H^+ ions from 0.5 g of the cation exchanger are 0.5 M and 190 mL, respectively. Further, the presence of Na^+ ions on the exchanger was confirmed by the EDX spectrum (Figure 3B). Based on the EDX data, no transmetalation or Ti washout occurred during ion exchange, confirming Ti-ATMP to be a rigid framework.

When in use, ion exchangers are subjected to a variety of physical and chemical effects that cause a loss of capacity, physical weakening of the exchange material, and partial solubilization. An evaluation of the chemical stability of ion-exchange materials in mineral acids, bases, and organic solvents is both useful and important for materials intended for various applications in varied environments. Ti-ATMP was found to be stable in acid and organic solvent media. It was not found to be as stable in base media. The maximum tolerable limits in these media are presented in Table 1.

The FTIR spectrum of Ti-ATMP (Supporting Information, Figure S3) exhibits a broad band in the range of ∼3400 cm^{-1} that is attributed to symmetric and asymmetric O−−H stretching vibrations due to residual water and the presence of structural hydroxyl groups, with H^+ corresponding to the —OH groups being cation-exchange sites. These sites are also referred to as defective P—OH groups.[45] A sharp medium band at ∼1636 cm^{-1} is attributed to aquo H—O—H bending.[46] The broad band at ∼1034 cm^{-1} is attributed to P—O—CH_2 stretching. The band at ∼1428 cm^{-1} is due to overlapping C−H bending of —CH_2 groups, P—C stretching vibrations, and the presence of tertiary amine groups.[31] The band at ∼722 cm^{-1} is attributed to metal oxide (Ti═O) bond.[36]

The TGA results reveal two regions of weight loss (Supporting Information, Figure S4). The first weight loss of ∼12% in the temperature range of 30−150 °C is attributed to the loss of moisture/hydrated water, whereas the second weight loss of ∼15% in the temperature range of 150−540 °C is attributed to the condensation of structural hydroxyl groups and decomposition of the organic moiety. The thermal behavior of the material was further investigated through the effect of calcination on the CEC (Table 1). It was observed that the CEC values decreased as the calcination temperature increased. The decrease in the CEC in the temperature range of 100−200 °C could be attributed to the loss of moisture and hydrated water. Further, the decrease in CEC beyond 200 °C could be attributed to the condensation of structural hydroxyl groups and decomposition of the organic moiety.

The absence of any sharp peaks in the X-ray diffractogram of Ti-ATMP indicates that Ti-ATMP is an amorphous material. The SEM image of Ti-ATMP (Supporting Information, Figure S5) shows the irregular morphology of the material.

3.2. Thermodynamics of Ion Exchange. The thermodynamics of ion exchange was studied for transition-metal ions Cu^{2+}, Zn^{2+}, Co^{2+}, and Ni^{2+} and heavy-metal ions Pb^{2+}, Cd^{2+}, and Hg^{2+}, and parameters such as the equilibrium constant (K), standard Gibbs free energy ($\Delta G°$), enthalpy ($\Delta H°$), and entropy ($\Delta S°$) were evaluated using standard equations[42,43] (see Table 2). A negative $\Delta G°$ value indicates that an exchange process is feasible and spontaneous in nature. A negative enthalpy change ($\Delta H°$) indicates that the exchange reaction is

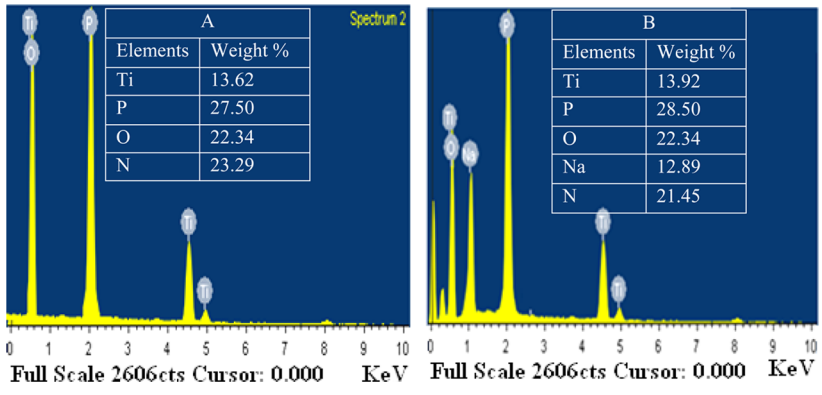

Figure 3. EDX spectra of (A) Ti-ATMP and (B) Na^+-exchanged Ti-ATMP.

dx.doi.org/10.1021/ie502673m | Ind. Eng. Chem. Res. 2014, 53, 17454−17467

Table 2. Thermodynamic Parameters Evaluated for $M^{2+}-H^{+}$ Exchange at Various Temperatures Using Ti-ATMP

metal ion	temperature (K)	K	$\Delta G°$ (kJ·mol^{-1})	$\Delta H°$ (kJ·mol^{-1})	$\Delta S°$ (J·mol^{-1}·°C^{-1})
Co^{2+}	303	1.77	−3.4	17.07	67.8
	313	1.98	−3.8		66.9
	323	2.35	−4.4		66.8
	333	2.39	−4.6		65.3
Ni^{2+}	303	1.23	−2.8	8.95	38.8
	313	1.38	−3.0		38.5
	323	1.40	−3.2		37.7
	333	1.55	−3.5		37.5
Cu^{2+}	303	2.96	−4.9	151.07	514.9
	313	3.12	−5.3		499.6
	323	4.02	−6.7		488.4
	333	8.1	−12.9		491.3
Zn^{2+}	303	1.52	−3.1	23.17	86.9
	313	1.98	−3.8		86.3
	323	2.29	−4.4		85.3
	333	2.37	−4.6		83.5
Cd^{2+}	303	0.36	1.29	49.24	155.6
	313	1.45	−0.48		153.9
	323	1.58	−0.61		190.2
	333	1.93	−0.91		197.1
Hg^{2+}	303	1.13	−0.15	12.04	25.0
	313	1.48	−0.51		36.9
	323	1.68	−0.70		39.7
	333	1.95	−0.92		40.2
Pb^{2+}	303	4.31	−6.6	139.01	481.0
	313	5.5	−8.4		471.3
	323	6.9	−10.6		463.3
	333	9.2	−14.1		460.0

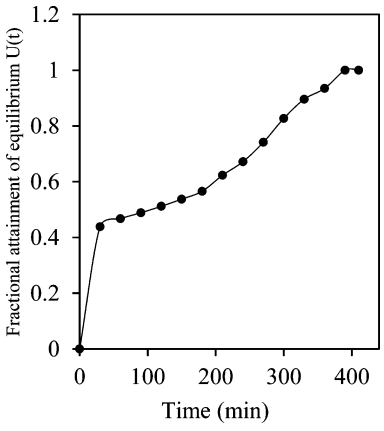

Figure 4. Fractional attainment of equilibrium for $Cu^{2+}-H^{+}$ exchange vs time using Ti-ATMP.

Table 4. Percentage Uptake of Metal Ions at Varying pH Using Ti-ATMP[a]

	uptake of metal ion (%)						
pH	Co^{2+}	Ni^{2+}	Cu^{2+}	Zn^{2+}	Cd^{2+}	Hg^{2+}	Pb^{2+}
1	11.54	7.88	17.78	37.93	16.67	3.85	17.78
2	19.28	7.06	36.00	42.50	28.00	19.28	28.00
3	29.55	13.19	**68.69**	46.77	**52.53**	**32.95**	35.35
4	44.00	18.95	55.45	**56.30**	44.55	22.00	**69.31**
5	**49.00**	**29.00**	45.10	45.24	34.31	18.00	34.31
6	41.00	23.00	34.95	43.17	25.24	11.00	22.33
7	37.00	–	–	–	–	5.00	–

[a]Maximum deviation in percentage uptake of metal ion = ±2%. Bold text in table indicates maximum uptake of metal ion at particular pH of solution.

exothermic, and a positive enthalpy change indicates that the exchange reaction is endothermic. The enthalpy change ($\Delta H°$) for an ion-exchange reaction can be either as a result of the net

Table 3. Kinetic Parameters Evaluated for $M^{2+}-H^{+}$ Exchange Using Ti-ATMP

	equilibrium values (mequiv·g^{-1})							
exchanging ion	303 K	313 K	323 K	333 K	ionic radius (Å)	D_0 (m^2·s^{-1})	E_a (kJ·mol^{-1})	ΔS^* (J·mol^{-1}·°C^{-1})
Co^{2+}	0.49	0.53	0.56	0.60	0.72	1.90×10^{-9}	10.67	−65.38
Ni^{2+}	0.47	0.50	0.52	0.54	0.72	1.48×10^{-9}	7.82	−78.43
Cu^{2+}	0.54	0.63	0.70	0.75	0.74	3.09×10^{-9}	23.99	−21.41
Zn^{2+}	0.55	0.58	0.62	0.65	0.74	2.94×10^{-9}	11.94	−63.30
Cd^{2+}	0.33	0.35	0.39	0.43	0.97	2.04×10^{-8}	18.95	−43.60
Hg^{2+}	0.28	0.21	0.33	0.49	1.10	1.09×10^{-8}	12.91	−69.37
Pb^{2+}	0.42	0.46	0.53	0.57	1.44	9.20×10^{-8}	25.48	−20.34

dx.doi.org/10.1021/ie502673m | Ind. Eng. Chem. Res. 2014, 53, 17454−17467

Table 5. Langmuir and Fruendlich Constants Evaluated for Transition- and Heavy-Metal Ions Using Ti-ATMP

		Langmuir constants				Fruendlich constants		
metal ion	temperature (K)	R^2	b ($dm^3 \cdot mg^{-1}$)	V_m ($mg \cdot g^{-1}$)	R_L	R^2	K	$1/n$
Co^{2+}	303	0.994	0.0076	12.95	0.992	0.990	4.520	0.655
	313	0.980	0.0061	15.36	0.999	0.994	3.799	0.579
	323	0.960	0.0052	20.08	0.992	0.979	3.751	0.574
	333	0.998	0.0062	21.09	0.999	0.993	3.415	0.533
Ni^{2+}	303	0.997	0.0018	15.77	0.999	0.992	2.512	0.689
	313	0.992	0.0034	17.57	0.992	0.996	4.501	0.568
	323	0.994	0.0045	18.11	0.991	0.999	1.148	0.824
	333	0.992	0.0098	18.31	0.991	0.991	9.232	0.395
Cu^{2+}	303	0.993	0.0024	21.05	0.993	0.997	5.204	0.716
	313	0.987	0.0024	29.23	0.992	0.996	5.984	0.777
	323	0.992	0.0036	38.02	0.992	0.988	5.000	0.699
	333	0.997	0.0020	68.51	0.999	0.992	4.742	0.676
Zn^{2+}	303	0.987	0.0026	16.75	0.999	0.992	3.157	0.791
	313	0.996	0.0047	19.45	0.999	0.935	2.891	0.895
	323	0.991	0.0073	20.00	0.999	0.932	2.841	0.926
	333	0.990	0.0081	39.57	0.991	0.982	4.137	0.616
Cd^{2+}	303	0.992	0.0020	22.07	0.993	0.948	3.061	0.485
	313	0.959	0.0016	41.66	0.991	0.989	2.903	0.462
	323	0.972	0.0017	47.61	0.996	0.916	2.646	0.422
	333	0.992	0.0021	50.00	0.992	0.891	2.655	0.424
Hg^{2+}	303	0.941	0.0039	23.25	0.997	0.961	3.784	0.578
	313	0.972	0.0052	22.72	0.996	0.973	3.380	0.529
	323	0.905	0.0036	35.71	0.992	0.976	4.246	0.628
	333	0.990	0.0041	43.47	0.991	0.998	6.368	0.804
Pb^{2+}	303	0.994	0.0104	46.51	0.993	0.995	2.486	0.231
	313	0.995	0.0121	56.81	0.991	0.962	3.091	0.232
	323	0.993	0.0628	57.14	0.993	0.938	3.823	0.184
	333	0.992	0.1485	60.24	0.999	0.991	4.196	0.175

Table 6. BTC and K_d Evaluated in Aqueous and Various Electrolyte Media Using Ti-ATMP[a]

		K_d ($mL \cdot g^{-1}$)								
			NH_4NO_3		HNO_3		$HClO_4$		CH_3COOH	
metal ion	BTC ($mmol \cdot g^{-1}$)	DIW[b]	0.02 M	0.2 M	0.02 M	0.2 M	0.02 M	0.2 M	0.02 M	0.2 M
Co^{2+}	0.51	2630	2501	435	681	630	879	170	730	69
Ni^{2+}	0.32	2390	1260	498	460	70	729	40	3075	2740
Cu^{2+}	0.72	19820	5539	3190	1498	129	1290	169	4780	4290
Zn^{2+}	0.56	3280	3229	1029	780	679	910	360	9230	4330
Cd^{2+}	0.21	2340	3989	2190	1820	1690	1480	559	1890	2298
Hg^{2+}	0.08	610	249	79	295	104	332	121	250	69
Pb^{2+}	0.40	3590	2698	2198	4479	224	4021	1169	7612	5190

[a]Values obtained under optimum conditions (optimum metal-ion concentration, optimum solution pH, and maximum equilibrium time). [b]DIW = deionized water.

effect of the following factors: (1) the heat consumed in bond breaking, as H^+ is released from the resin; (2) the heat released in the formation of bonds with the incoming cation; (3) the heat corresponding to the energy required for crossing the barrier (distance between the exchange phase and the solution phase); and (4) the enthalpy change accompanying hydration and dehydration of the exchanging ions in solution. The entropy change (ΔS°) normally depends on the extent of hydration of the exchangeable and exchanging ions, along with any change in water structure around ions that might occur when they pass through the channels of the exchanger, introducing a high degree of disorder into the resin matrix as a result of the ion-exchange process.

A plot of the fractional attainment of equilibrium [$U(t)$] versus time (t) (Figure 4) shows that the exchange equilibrium for Ti-ATMP was apparently attained within 6 h, and hence, all of the equilibrium studies were performed after the samples had been shaken for 6 h. The equilibrium constant (K) was found to increase with increasing temperature for all metal ions under study (Table 2), indicating that the metal ions have a high affinity for the exchanger and that the mechanism is ion exchange. In the present study, ΔG° for all metal exchange reactions was found to be negative over the entire temperature range, indicating that the exchanger has a greater preference for metal ions than H^+ ions. The ΔG° values became more negative with increasing temperature, confirming that the exchange was favored with increasing temperature. ΔH° was positive in all cases, indicating the process to be endothermic. Higher/positive values of enthalpy change indicate more endothermicity of the exchange process and the requirement

dx.doi.org/10.1021/ie502673m | Ind. Eng. Chem. Res. 2014, 53, 17454−17467

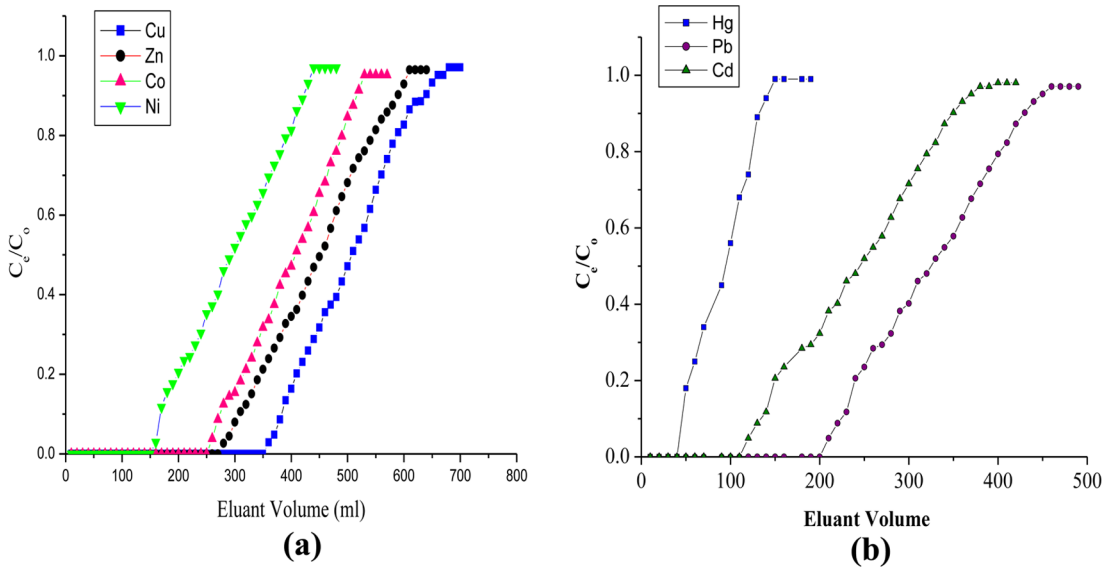

Figure 5. BTCs of (a) transition-metal and (b) heavy-metal ions using Ti-ATMP.

Table 7. Comparison of Cation-Exchange Capacities of Ti-ATMP and Other M(IV) Phosphonates

compound[a]	CEC (mequiv·g^{-1})
Ti-ATMP	4.01
Zr-ATMP	3.61
Zr-DETPMP	2.34
Zr-HEDP	3.18
Ti-DETPMP	3.56

[a]ATMP = amino tris(methylene phosphonic acid), HEDP = hydroxyethylidene diphosphonic acid, DETPMP = diethylene triamine penta(methylene phosphonic acid).

of more energy for dehydration to occur. As dehydration is a must for ion exchange to occur, some energy must be supplied to the cation as it leaves the hydration sphere to undergo ion exchange.[47] The $\Delta H°$ values indicate that complete dehydration probably occurs in the cases of Cu^{2+} among transition-metal ions and Pb^{2+} among heavy-metal ions. These observations are in keeping with high negative $\Delta G°$ values for Cu^{2+} and Pb^{2+}. $\Delta S°$ also follows same trend as $\Delta H°$ for all metal ions. The higher $\Delta S°$ values also observed for Cu^{2+} and Pb^{2+} are attributed to greater dehydration, which indicates greater disorder produced during the exchange.

3.3. Kinetic Study. It is well established that the rate-determining step in an ion-exchange process is the interdiffusion of counterions. The rate-controlling mechanism can be film diffusion or particle diffusion. Ion exchange was studied at 303 K for varying metal-ion concentrations, and the effect of reaction temperature on ion exchange was studied in the temperature range of 303−333 K in 10 K intervals for the different transition-metal ions Cu^{2+}, Zn^{2+}, Ni^{2+}, and Co^{2+} and heavy-metal ions Pb^{2+}, Cd^{2+}, and Hg^{2+}. A representative plot of τ (dimensionless time parameter, determined by fractional attainment of equlibrium) versus t for the Cu^{2+}−H^+ exchange process is presented in Figure S6 (Supporting Information). For metal-ion concentrations greater than or equal to 0.014 M, straight lines passing through the origin were obtained, confirming a particle-diffusion-controlled exchange at these concentrations.[48] For further kinetic studies, this minimum concentration (0.014 M for the M^{2+}−H^+ exchange process) was taken, because at this concentration, Donnan exclusion is predominant, which prevents the interference of co-ions in the exchange process.[43] A plot of τ versus t (Figure S7, Supporting Information) for Cu^{2+}−H^+ exchange at different temperatures was found to be linear; similar results were obtained for the other metal ions. From the slope (S) of the τ versus t plots, values of D_A were calculated using the relationship $D_A = Sr_0^2$, where S is the slope (obtained from τ versus t) and r_0 is the bead radius (radius of the exchanger particles). It can be observed from Figure S8 (Supporting Information) that a plot of ln D_A (diffusion coefficient of counter ion A) versus $1/T$ is linear for Cu^{2+}, verifying the validity of the Arrhenius relation, $D_A = D_0 \exp(-E_a/RT)$; similar observations were made for the

Table 8. Percentage Elution (E, %) of Metal Ions in Various Electrolyte Media Using Ti-ATMP[a]

	NH_4NO_3		HNO_3		$HClO_4$		CH_3COOH	
metal ion	0.02 M	0.2 M	0.02 M	0.2 M	0.02 M	0.2 M	0.02 M	0.2 M
Co^{2+}	91	94	91	95	90	94	95	96
Ni^{2+}	93	98	94	99	91	94	98	99
Cu^{2+}	86	91	88	90	89	90	70	75
Zn^{2+}	82	90	89	92	88	90	90	89
Cd^{2+}	89	93	95	96	86	91	91	92
Hg^{2+}	98	97	98	99	94	98	95	98
Pb^{2+}	89	90	87	90	85	88	87	88

[a]Eluent volume = 60 and 50 mL for 0.02 and 0.2 M electrolytes, respectively, Maximum deviation in percentage elution of metal ions = ±2.

dx.doi.org/10.1021/ie502673m | Ind. Eng. Chem. Res. 2014, 53, 17454−17467

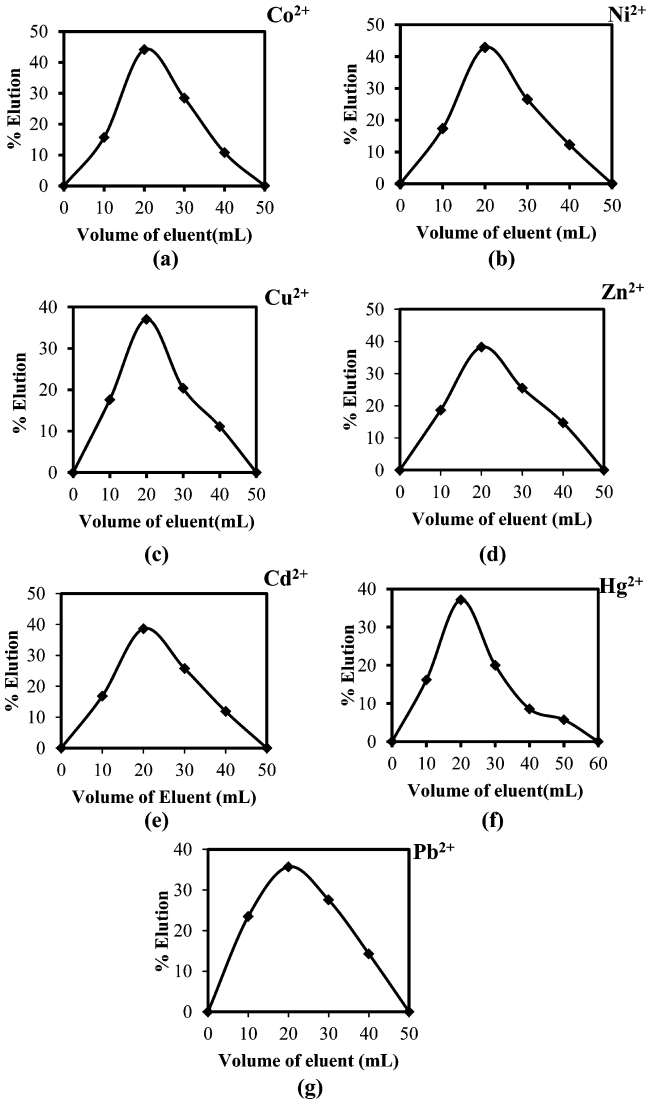

Figure 6. Elution behavior of transition- and heavy-metal ions using 0.2 M HNO_3 as the eluent: (a) Co^{2+}, (b) Ni^{2+}, (c) Cu^{2+}, (d) Zn^{2+}, (e) Cd^{2+}, (f) Hg^{2+}, and (g) Pb^{2+} using Ti-ATMP.

other metal ions. The energy of activation (E_a) and the pre-exponential constant (D_0) were evaluated from the slope and intercept of these plots. The entropy of activation (ΔS^*) was then calculated using the equation $D_0 = 2.72d^2(kT/h)\exp(\Delta S^*/R)$, where d is the average distance between two exchanging sites (taken as 5 Å) and the other terms have their usual meanings.[48,49] Because the exchanger is not dynamic, the ion-exchange process depends on the mobility of the exchanging ions. The self-diffusion coefficient (D_0) gives an idea of the mobility of the migrating ions and depends on the size and charge of the ion and on the extent of hydration in aqueous medium. During the exchange, the orientations of the exchanger sites and mobile ions are equally important, and this aspect of the process is expressed as an orientation factor. Because it is related to randomness, the orientation factor is given by the entropy of activation (ΔS^*). The overall rate of exchange reaction thus depends on D_0, E_a, and ΔS^*. It is thus expected that larger values of D_0 and ΔS^* and smaller values of E_a indicate a higher rate of exchange. The values of the self-diffusion coefficient (D_0), energy of activation (E_a), and entropy of activation (ΔS^*) are summarized in Table 3. From this table, it can be seen that, for all of the metal ions under study in this work, the equilibrium values increased with increasing temperature. This might be due to an increase in the mobility of the ions with increasing temperature.

In the present study, the observed order for D_0, E_a, and ΔS^* was $Cu^{2+} > Zn^{2+} > Co^{2+} > Ni^{2+}$ (for transition-metal ions) and $Pb^{2+} > Cd^{2+} > Hg^{2+}$ (for heavy-metal ions). Among the transition-metal ions, the sizes are in the order $Cu^{2+} \approx Zn^{2+} > Co^{2+} \approx Ni^{2+}$. Cu^{2+} and Zn^{2+}, having larger ionic radii, are less hydrated, and thus, their self-diffusion coefficients should be higher than those of Co^{2+} and Ni^{2+}, which is in accordance with the observed order. The sizes of heavy-metal ions follow the order $Pb^{2+} > Hg^{2+} > Cd^{2+}$. As larger ions are less hydrated, the self-diffusion coefficient of Pb^{2+} is highest. The order of self-diffusion coefficients should be $Pb^{2+} > Hg^{2+} > Cd^{2+}$. However, in the present study, the observed order for D_0 was $Pb^{2+} > Cd^{2+} > Hg^{2+}$. Other factors that contribute to self-diffusion coefficients include electrostatic interactions of the metal ions with the exchange sites, which increase with increasing charge density,[50] site acidity, pore size, and size of the exchanger particle, which could be the decisive factors in certain cases.[51] The D_0 order found in this work is due to the net contributions of all of these factors.

For an ion exchanger, E_a values depend on the ease of dehydration of a hydrated ion, for it to occupy a site on the exchanger. Based on ion size, E_a should follow the order $Co^{2+} \approx Ni^{2+} > Cu^{2+} \approx Zn^{2+}$ and $Cd^{2+} > Hg^{2+} > Pb^{2+}$. However, in the present study, the observed order of E_a was $Cu^{2+} > Zn^{2+} > Co^{2+} > Ni^{2+}$ for transition-metal ions and $Pb^{2+} > Cd^{2+} > Hg^{2+}$ for heavy-metal ions, falling in the range 7.82−23.99 kJ mol^{-1} for transition-metal ions and 12.91−25.48 kJ mol^{-1} for heavy-metal ions. The apparently low values indicate low diffusion barriers for the metal ions when they pass through the structural channels during ion exchange. The low E_a values are also indicative of the fact that the metal-ion exchange studied herein is diffusion-controlled, as observed earlier.[52] E_a values also depend on several other factors such as coulombic barrier, geometry of exchanger particle, and charge of the incoming ions. E_a values also reflect the ΔH values, which follow the same order. The same reasons can be forwarded as in section 3.2. The overall E_a values are the results of contributions of the above-mentioned factors.

The entropy reflects changes in the hydration sphere of the exchanging cation during the ion-exchange process. When ion exchange occurs, a cation of high entropy in the external aqueous phase becomes a cation of lower entropy in the exchanger phase, which results in a significant negative contribution to the entropy change. In the present study, the entropy of activation, ΔS^*, was found to be negative for both transition-metal and heavy-metal ions (Table 3). Negative values of ΔS^* indicate decreases in the degree of randomness at the surface of the exchanger during the metal-ion-exchange process.

3.4. Adsorption Studies. The effects of experimental conditions such as pH, contact time, and temperature were studied to determine the conditions for the maximum sorption/ion exchange of the metal ions by the ion exchanger.

At pH values of less than ∼3, very little sorption was observed for all metal ions (Table 4). The lack of sorption at low pH can be attributed to the high concentration of hydrogen ions competing with the metal ions for sorption/exchange sites. The effects of contact time and reaction temperature on the percentage uptake of metal ion are presented in Table 4. It can

dx.doi.org/10.1021/ie502673m | Ind. Eng. Chem. Res. 2014, 53, 17454−17467

Table 9. Binary and Ternary Separations of Transition- and Heavy-Metal Ions Using Ti-ATMP

metal-ion pairs	eluents	amount of metal ion loaded (mg)	amount of metal ion eluted (mg)	elution[a] (%)
Ni^{2+}–Cu^{2+}	(a) 0.2 M $HClO_4$ (Ni^{2+})	0.5893	0.5375	91
	(b) 0.2 M HNO_3 (Cu^{2+})	0.6354	0.5097	80
Co^{2+}–Cu^{2+}	(a) 0.2 M CH_3COOH (Co^{2+})	0.5869	0.5211	88
	(b) 0.2 M HNO_3 (Cu^{2+})	0.6354	0.4477	70
Zn^{2+}–Cu^{2+}	(a) 0.2 M $HClO_4$ (Zn^{2+})	0.6539	0.5434	83
	(b) 0.2 M HNO_3 (Cu^{2+})	0.6354	0.4445	69
Ni^{2+}–Zn^{2+}	(a) 0.2 M $HClO_4$ (Ni^{2+})	0.5893	0.5485	93
	(b) 0.2 M NH_4NO_3 (Zn^{2+})	0.6539	0.5534	84
Hg^{2+}–Cd^{2+}	(a) 0.2 M NH_4NO_3(Hg^{2+})	2.0059	1.8973	94
	b)0.2 M $HClO_4$(Cd^{2+})	1.1241	0.9878	87
Cd^{2+}–Pb^{2+}	a)0.2 M $HClO_4$(Cd^{2+})	1.1241	0.9728	86
	(b) 0.2 M HNO_3 (Pb^{2+})	2.0720	1.3465	64
Hg^{2+}–Pb^{2+}	(a) 0.2 M NH_4NO_3 (Hg^{2+})	2.0059	1.9179	95
	(b) 0.2 M HNO_3 (Pb^{2+})	2.0720	1.5647	75
Ni^{2+}–Co^{2+}–Cu^{2+}	(a) 0.2 M $HClO_4$ (Ni^{2+})	0.5893	0.4132	70
	(b) 0.2 M CH_3COOH (Co^{2+})	0.5869	0.3954	67
	(c) 0.2 M HNO_3 (Cu^{2+})	0.6354	0.3494	55
Hg^{2+}–Cd^{2+}–Pb^{2+}	(a) 0.2 M NH_4NO_3 (Hg^{2+})	2.0059	1.4400	72
	(b) 0.2 M $HClO_4$(Cd^{2+})	1.1241	0.7808	69
	(c) 0.2 M HNO_3 (Pb^{2+})	2.0720	1.2639	61

[a]Maximum deviation in percentage elution = ±2.

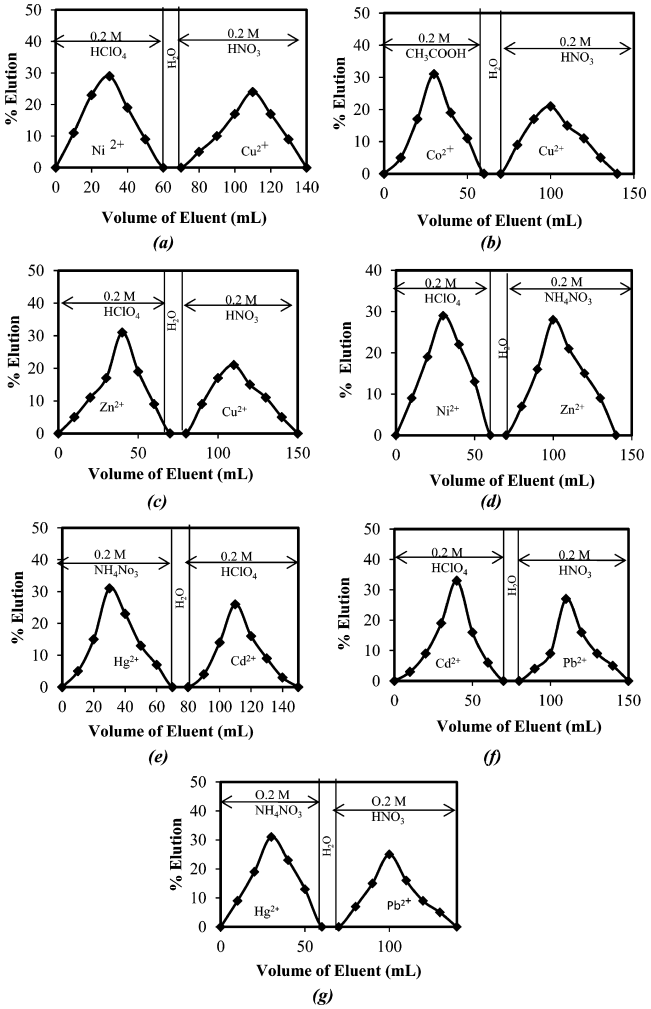

Figure 7. Binary separations of transition- and heavy-metal ions using Ti-ATMP: (a) Ni^{2+}–Cu^{2+}, (b) Co^{2+}–Cu^{2+}, (c) Zn^{2+}–Cu^{2}, (d) Ni^{2+}–Zn^{2+}, (e) Hg^{2+}–Cd^{2+}, (f) Cd^{2+}–Pb^{2+}, and (g) Hg^{2+}–Pb^{2+}.

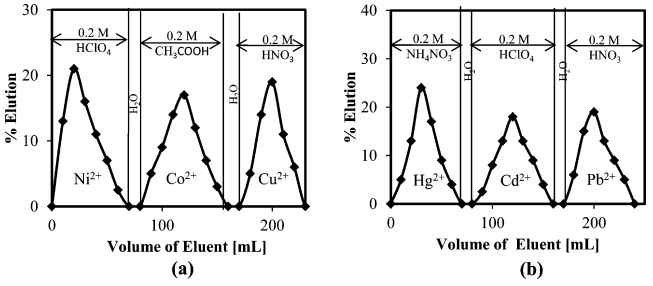

Figure 8. Ternary separations of transition- and heavy-metal ions using Ti-ATMP: (a) Ni^{2+}–Co^{2+}–Cu^{2+} and (b) Hg^{2+}–Cd^{2+}–Pb^{2+}.

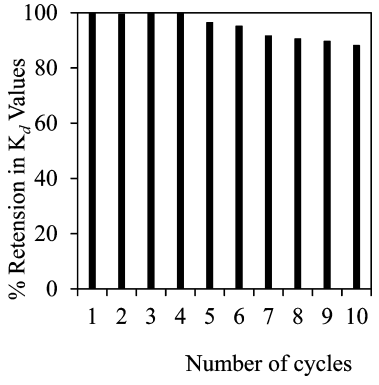

Figure 9. Plot of percentage retention in K_d value vs number of cycles using Ti-ATMP.

observed that sorption increased gradually with increasing contact time and reached a maximum value, after which randomness was observed. The increase in percentage uptake can be attributed to two different sorption processes, namely, a fast ion exchange followed by chemisorption.[53] It was observed that the uptake of each metal ion increased with increasing temperature, which indicates the uptake to be an ion-exchange mechanism. The percentage uptake was calculated as $[(C_0 - C_e)/C_0] \times 100$, where C_0 is the initial concentration of metal

dx.doi.org/10.1021/ie502673m | Ind. Eng. Chem. Res. 2014, 53, 17454–17467

ion in mg/L and C_e is the final concentration of metal ion in mg/L. The time taken for the attainment of equilibrium for transition-metal ions was ~50−150 min, and that for heavy-metal ions was ~50−110 min (Supporting Information, Table S2).

Equilibrium behavior is described in terms of equilibrium isotherms, which depend on the system temperature, solution concentration, contact time, and pH.[54] Adsorption equilibrium is usually established when the concentration of an adsorbate (metal ions) in a bulk solution is in dynamic balance with that on the adsorbent (exchanger) interface. The variation in adsorption with concentration and temperature is generally expressed in terms of adsorption isotherms, in this case, the Langmuir and Freundlich adsorption isotherms.

The linearized form of the Langmuir isotherm equation is given by $C_e/(X/m) = 1/(bV_m) + C_e/V_m$, where X is the amount of adsorbate, m is the amount of adsorbent, and C_e is the equilibrium concentration of the adsorbate in the solution. b is a constant that represents the adsorption bond energy, which is related to the affinity between the adsorbent and adsorbate. It is also a direct measure of the intensity of the sorption process. V_m is a constant related to the area occupied by a monolayer of sorbate, reflecting the maximum adsorption capacity.[54] A dimensionless constant equilibrium parameter R_L can also be used to express an essential characteristic of the Langmuir isotherm. The R_L value indicates the shape of the isotherm and is expressed by the equation $R_L = 1/(1 + bC_0)$. A value in the range $0 < R_L < 1$ indicates favorable adsorption, $R_L = 0$ indicates irreversible adsorption, $R_L = 1$ means linear adsorption, and a value of $R_L > 1$ indicates unfavorable adsorption.[54]

The Freundlich isotherm is expressed as $\log(X/m) = \log K + (1/n) \log C_e$, where X and m have the same meanings as for the Langmuir isotherm and K and $1/n$ are the Fruendlich constants, describing the adsorption capacity and intensity, respectively. A value in the range of $0 < 1/n < 1$ indicates a normal isotherm, whereas $1/n > 1$ indicates cooperative sorption, and for $n = 1$, the partition between the two phases is independent of the concentration.[55]

The isotherm constants are important in understanding the adsorption mechanism and their subsequent application for the prediction of some important design parameters. Plots of $C_e/(X/m)$ versus C_e and $\log(X/m)$ versus $\log C_e$ are constructed for the Langmuir and Freundlich isotherms, respectively, which form straight lines from which the constants can be determined from the slopes and intercepts. To determine which type of isotherm fits the data better, the R^2 values (goodness-of-fit criterion) were computed by linear regression for both type of isotherms. A value in the range $0 < R^2 < 1$ indicates that the isotherm provides a good fit to the sorption experimental data, where R^2 values should be close to unity.

The Langmuir constants (b and V_m) and Freundlich constants (K and $1/n$) obtained from the slopes and intercepts of the linear plots are listed in Table 5. The values of R^2 show that the Langmuir and Freundlich isotherms both provide good fits to the experimental data, where the R^2 close to unity indicate that both isotherms are appropriate for the sorption of all of the metal ions under study in this work. Variation in R^2 values is attributed to the fact that the surface adsorption is not adsorption of a monolayer with a single type of adsorption site. Two or more sites with different affinities might be involved in metal-ion sorption. In the present study, low values of b indicate favorable adsorption. The V_m values, which indicate the maximum adsorption capacities of the exchanger for the metal ions, follow the order $Cu^{2+} > Zn^{2+} > Co^{2+} > Ni^{2+}$ among transition-metal ions and $Pb^{2+} > Cd^{2+} > Hg^{2+}$ among heavy-metal ions at 303 K. The values of $1/n$ and R_L were obtained between 0 and 1, which indicate normal isotherms and favorable adsorption, respectively, and agree with reported results.[54,55]

3.5. Distribution Studies and Breakthrough Capacity (BTC). The effects of the metal-ion concentration on K_d were investigated (Supporting Information, Table S3), and it was found that the K_d values increased with increasing concentration. Above a particular concentration, the K_d values became constant, which can be explained by the fact that, at lower concentrations, almost all of the ions were exchanged because of the availability of exchangeable sites, which were not available at higher concentrations. The optimum concentrations are reported in Table S3 (Supporting Information).

The K_d values determined for the metal ions studied in this work under the optimum conditions (optimum metal-ion concentration, pH of maximum adsorption, and maximum equilibrium time) using Ti-ATMP are presented in Table 6. In general, it can be observed that the K_d values were lower at high electrolyte concentrations and vice versa. In strong electrolyte media, the K_d values were lower than in weak electrolyte and aqueous media. This can be attributed to the high competition among ions for exchange in strong electrolyte media. The K_d values in aqueous medium follow the order $Cu^{2+} > Zn^{2+} > Co^{2+} > Ni^{2+}$ among transition-metal ions and $Pb^{2+} > Cd^{2+} > Hg^{2+}$ among heavy-metal ions. The most promising features of Ti-ATMP are the high K_d values observed for Cu^{2+} and Pb^{2+} (aqueous medium), whereas Ni^{2+} and Hg^{2+} exhibit very low K_d values in 0.2 M $HClO_4$, 0.2 M CH_3COOH, and 0.2 M NH_4NO_3.

Breakthrough curves (plots of C_e/C_0 versus effluent volume) are presented in Figure 5. Breakthrough capacity (BTC) is the dynamic capacity or operating capacity of a known amount of ion-exchange material toward a metal ion in column operation. In a dynamic process, the exchange of a particular metal ion depends mainly on the rate of exchange, contact time, flow rate of feed solution through the column, bed depth, selectivity coefficient, particle size, and temperature. K_d values also give an idea of the affinity of a metal ion toward the ion exchanger, which is determined by a batch process. It is expected that the metal-ion affinities toward an exchanger based on K_d and BTC should be same, as was observed (Table 6) in the present study.

3.6. Summarizing Ion-Exchange Behavior of Ti-ATMP. In the present study, the obtained metal phosphonate Ti-ATMP exhibited much higher CEC values than other metal phosphonates reported by us earlier (Table 7). Further, from the above discussion, it can be observed that K_d, BTC, and V_m (maximum adsorption capacity) follow the same order as the metal-ion affinity toward Ti-ATMP, namely, $Cu^{2+} > Zn^{2+} > Co^{2+} > Ni^{2+}$ among the transition-metal ions and $Pb^{2+} > Cd^{2+} > Hg^{2+}$ among the heavy-metal ions. This is also well supported by the thermodynamic parameters determined in this work. A higher negative value of ΔG° indicates feasibility and spontaneity of ion exchange, whereas a higher positive value of ΔH° indicates endothermicity due to greater dehydration of a metal ion to occupy a site on the exchanger, for which energy must be supplied. This is followed by a higher positive value of ΔS° attributed to randomness due to the high degree of disorder introduced into the resin matrix through the ion-

exchange process. Thus, $\Delta G°$, $\Delta H°$, and $\Delta S°$ also support the observed trends.

3.7. Elution and Separation Studies. The elution behaviors of transition-metal ions and heavy-metal ions (under study) were studied using different electrolytes such as HNO_3, $HClO_4$, CH_3COOH, and NH_4NO_3 at concentrations of 0.02 and 0.2 M, and the results are presented in Table 8. The percentages of metal eluted in all cases were in the range of 70−99%. Good elution was observed due to the presence of a single metal ion and the noninterference of other elements. In general, higher concentrations and acids are better eluants. The best eluant for most metal ions was found to be 0.2 M HNO_3. Using 0.2 M HNO_3, order of the percentages of metal eluted among the transition-metal ions was Ni^{2+} (99%) > Co^{2+} (95%) > Zn^{2+} (92%) > Cu^{2+} (90%), and that among the heavy-metal ions was Hg^{2+} (99%) > Cd^{2+} (96%) > Pb^{2+} (90%). These observations are in keeping with the fact that metal ions with high K_d values are less eluted and vice versa. All elution curves (Figure 6) exhibited symmetrical bell shapes, indicating elution efficiency.

The separation factor α, the rate at which two constituents separate on a column, which is given by $\alpha = K_{d1}/K_{d2}$, where K_{d1} and K_{d2} are the distribution coefficients of the two constituents being separated, provides a guideline for metal separation. The greater the deviation of α from unity, the better the separation. The efficiency of an ion-exchange separation depends on the conditions under which α has a useful value or influences the system in a direction favorable to separation. For a given metal-ion pair, the electrolyte medium in which the separation factor is the highest is selected as the eluent. Thus, a study on the distribution behavior of metal ions in various electrolyte media provides an idea about the eluents that can be used for separation.

Binary separations for the metal-ion pairs Ni^{2+}−Cu^{2+}, Co^{2+}−Cu^{2+}, Zn^{2+}−Cu^{2+}, Ni^{2+}−Zn^{2+}, Hg^{2}−Pb^{2+}, Cd^{2+}−Pb^{2+}, and Hg^{2+}−Cd^{2+} were performed using the concept of high separation factor in a particular medium, as discussed earlier in the text. In these binary separations, the separation efficiency was in the range of 69−93% among transition-metal ions and 64−95% among heavy-metal ions (Table 9). In all cases of binary separation, irrespective of the metal-ion pair, maximum percentages of metal eluted were 80% for Cu^{2+}, 84% for Zn^{2+}, 88% for Co^{2+}, and 93% for Ni^{2+} (93%) (among transition-metal ions) and 75% for Pb^{2+}, 87% for Cd^{2+}, and 95% for Hg^{2+} (among heavy-metal ions). These observations are in keeping with the separation factors (α) and K_d values of the metal ions. The percentage of metal eluted decreased with decreasing separation factor and increased with increasing separation factor, and as explained earlier, metal ions with high K_d values were less eluted and vice versa. Efficient separations in terms of percentages of metal eluted were observed and also supported by symmetrical bell-shaped curves (Figure 7).

In ternary separations of transition-metal ions Co^{2+}−Ni^{2+}−Cu^{2+} and heavy-metal ions Hg^{2+}−Cd^{2+}−Pb^{2+}, the percentages of metal eluted were in the ranges of 55−70% and 61−72%, respectively (Table 9). In all cases, three distinct peaks were observed (Figure 8), but with tailing effects for each metal ion eluted. The percentages of metal eluted were also lower as compared to those observed in single and binary metal-ion experiments. The separation process probably becomes complex, as a result of the loss of metal ions during the changeover of the eluent, interference of metal ions, pH, simultaneous elution of two or more metal ions with the same eluent, and experimental errors involved in the determination of metal ions in the presence of other ions.

3.8. Regeneration and Reuse of Ti-ATMP. A study on the regeneration and reuse of Ti-ATMP was performed as described in the Experimental Section. It was observed that the exchanger, once used, could be converted back to its original form by desorption of the metal ions with concentrated nitric acid. A plot of the percentage retention of K_d versus number of cycles is presented in Figure 9, which shows that the percentage retention of K_d was almost constant up to 5 cycles, indicating that Ti-ATMP could be regenerated and reused without much decline in performance.

4. CONCLUSIONS

Ti-ATMP exhibits promising ion-exchange characteristics, namely, good CECs, thermal stability, chemical stability, good regeneration capacity, and high affinity for Cu^{2+} and Pb^{2+}. The metal-ion affinity toward Ti-ATMP for transition-metal ions was found to be in the order Cu^{2+} > Zn^{2+} > Co^{2+} > Ni^{2+}, and that for heavy-metal ions was in the order Pb^{2+} > Cd^{2+} > Hg^{2+}, which was confirmed by the distribution coefficient (K_d), breakthrough capacity, and V_m values, which were well supported by the thermodynamic parameters evaluated. Efficient binary and ternary metal separations carried out using Ti-ATMP indicate good potential for this material to be used as a cation exchanger.

■ ASSOCIATED CONTENT

Supporting Information

Additional information as noted in text. This material is available free of charge via the Internet at http://pubs.acs.org.

■ AUTHOR INFORMATION

Corresponding Author

*Tel.: +91-9426344434. E-mail: uvcres@gmail.com.

Notes

The authors declare no competing financial interest.

■ ACKNOWLEDGMENTS

The authors thank M. S. University of Baroda for providing a research fellowship to B.S.

■ REFERENCES

(1) Singh, S.; Patel, P.; Shahi, V.; Chudasama, U. Pb^{2+} selective and highly cross-linked zirconium phosphonate membrane by sol−gel in aqueous media for electrochemical applications. *Desalination* **2011**, *276*, 175−183.

(2) Mahmoud, M.; Yakout, A.; Abdel-Aal, H.; Osman, M. High performance SiO_2-nanoparticles-immobilized-Penicillium funiculosum for bioaccumulation and solid phase extraction of lead. *Bioresour. Technol.* **2012**, *106*, 125−132.

(3) Mohamed, M.; Soliman, E.; Dlssouky, A. Metal Uptake Properties of Polystyrene Resin Immobilized Polyamine and Formylsalicylic Acid Derivatives as Chelation Ion Exchangers. *Anal. Sci.* **1997**, *13*, 765−769.

(4) Wang, Y. H.; Lin, S. H.; Juang, R. S. Removal of heavy metal ions from aqueous solutions using various low-cost adsorbents. *J. Hazard. Mater.* **2003**, *B102*, 291−302.

(5) Mahmoud, M.; Al-Bishri, H. Supported hydrophobic ionic liquid on nano-silica for adsorption of lead. *J. Chem. Eng.* **2011**, *166*, 157−167.

(6) Mahmoud, M.; Haggag, S.; Hegazi, A. Synthesis, characterization, and sorption properties of silica gel-immobilized pyrimidine derivative. *J. Colloid Interface Sci.* **2006**, *300*, 94−99.

(7) Mahmoud, M.; Al-bishri, H. Adjusted pH for the Selective Separation of Cadmium from Lead by Nano-Active Silica-Functionalized-[$Bmim^{+}Tf_2N^{-}$] Ionic Liquid. *Sep. Sci. Technol.* **2013**, *48*, 931−940.
(8) Mahmoud, M.; Masoud, M.; Maximous, N. Synthesis, Characterization and Selective Metal Binding Properties of Physically Adsorbed 2-Thiouracil on the Surface of Porous Silica and Alumina. *Microchim. Acta* **2004**, *147*, 111−115.
(9) Siddiqui, W. A.; Khan, S. A. Synthesis, characterization and ion exchange properties of zirconium(IV) tungstoiodophosphate, a new cation exchanger. *Bull. Mater. Sci.* **2007**, *30*, 43−49.
(10) Velmurugan, S.; Sathyaseelam V. S.; Narasimhan, S. V.; Mathur, P. K. In *New Developments in Ion Exchange: Materials, Fundamentals, and Applications: Proceedings of the International Conference on Ion Exchange (ICIE'91), Tokyo, Japan, October 2−4, 1991*; Abe, M., Kataoka, T., Suzuki, T., Eds.; Kodansha: Tokyo, Japan, 1991.
(11) Inamuddin; Khan, S. A.; Siddiqui, W. A.; Khan, A. A. Synthesis, characterization and ion-exchange properties of a new and novel 'organic−inorganic' hybrid cation-exchanger: Nylon-6,6, Zr(IV) phosphate. *Talanta* **2007**, *71*, 841−847.
(12) Siddiqui, W. A.; Khan, S. A.; Inamuddin. Synthesis, characterization and ion exchange properties of a new and novel 'organic−inorganic' hybrid cation-exchanger: Poly(methyl methacrylate) Zr(IV) phosphate. *Colloid. Surface. A* **2007**, *295*, 193−199.
(13) Ma, T. Y.; Zhang, X. J.; Shao, G. S.; Cao, J. L.; Yuan, Z. Y. Ordered macroporous titanium phosphonate materials: Synthesis, photocatalytic activity, and heavy metal ion adsorption. *J. Phys. Chem. C* **2008**, *112*, 3090−3096.
(14) Zhu, Y.; Ma, T.; Liu, Y.; Zhen Ren, T.; Yuan, Z. Metal phosphonate hybrid materials: From densely layered to hierarchically nanoporous structures. *Inorg. Chem. Front.* **2014**, *1*, 360−383.
(15) Chiang, C. L.; Chang, R. C.; Chiu, Y. C. Thermal stability and degradation kinetics of novel organic-inorganic epoxy hybrid containing nitrogen/silicon/phosphorous by sol−gel method. *Thermochim. Acta* **2007**, *453*, 97−104.
(16) Clearfield, A. *Inorganic Ion Exchange Materials*; CRC Press: Boca Raton, FL, 1982; pp 440−445.
(17) Varshney, K. G.; Khan, M. A. Amorphous Inorganic Ion Exchangers. In *Inorganic Ion Exchangers in Chemical Analysis*; Qureshi, M., Varshney, K. G., Eds.; CRC Press: Boca Raton, FL. 1991; Chapter 6, pp 177−270.
(18) Sahu, B. B.; Mishra, H. K.; Parida, K. Cation exchange and sorption properties of tin(IV) phosphate. *J. Colloid Interface Sci.* **2000**, *225*, 511−519.
(19) Maheria, K.; Chudasama, U. Synthesis and characterization of a new phase of titanium phosphate and its application in separation of metal ions. *Indian J. Chem. Technol.* **2007**, *14*, 423−426.
(20) Jayswal, A.; Chudasama, U. Synthesis and characterization of a new phase of zirconium phosphate for the separation of metal ions. *J. Iran. Chem. Soc.* **2007**, *4*, 510−515.
(21) Varshney, K. G.; Pandit, H. A. Thermodynamics of the Na(I)−H(I), K(I)−H(I), and Ca(II)−H(I) exchanges on zirconium(IV) aluminophosphate cation exchanger. *Colloids Surf. A: Physicochem. Eng. Aspects* **2002**, *201*, 1−7.
(22) Clearfield, A.; Wang, Z. J. Organically pillared microporous zirconium phosphonates. *J. Chem. Soc., Dalton Trans.* **2002**, *7*, 2937−2947.
(23) Clearfield, A. Metal Phosphonate Chemistry. In *Progress in Inorganic Chemistry*; Karlin, K. D., Ed.; John Wiley & Sons: New York, 1998; Vol. *47*, pp 371−510.
(24) Bauer, S.; Bein, T.; Stock, N. High-throughput investigation and characterization of cobalt carboxy phosphonates. *Inorg. Chem.* **2005**, *44*, 5882−5889.
(25) Gomez-Alcantara, M. M.; Cabeza, A.; Martinez-Lara, M.; Aranda, M. A. G.; Aarau, R.; Bhuvanesh, N.; Clearfield, A. Synthesis and characterization of a new bisphosphonic acid and several metal hybrids derivatives. *Inorg. Chem.* **2004**, *43*, 5283−5293.
(26) Clearfield, A. Recent advances in metal phosphonate chemistry. *Curr. Opin. Solid State Mater. Sci.* **1996**, *1*, 268−278.
(27) Zhu, Y.; Zhen Ren, T.; Yuan, Z. Mesoporous non-siliceous inorganic−organic hybrids: A promising platform for designing multifunctional materials. *New J. Chem.* **2014**, *38*, 1905−1922.
(28) Zhu, Y. P.; Ma, T. Y.; Ren, T. Z.; Li, J.; Du, G. H.; Yuan, Z. Y. Highly dispersed photoactive zinc oxide nanoparticles on mesoporous phosphonated titania hybrid. *Appl. Catal. B: Environ.* **2014**, *157*, 44−52.
(29) Ma, T. Y.; Lin, X. Z.; Zhang, X. J.; Yuan, Z. Y. High surface area titanium phosphonate materials with hierarchical porosity for multiphase adsorption. *New J. Chem.* **2010**, *34*, 1209−1216.
(30) Ma, T. Y.; Yuan, Z. Y. Functionalized periodic mesoporous titanium phosphonate monoliths with large ion exchange capacity. *Chem. Commun.* **2010**, *46*, 2325−2327.
(31) Ma, T. Y.; Lin, X. Z.; Zhang, X. J.; Yuan, Z. Y. Periodic mesoporous titanium phosphonate hybrid materials. *J. Mater. Chem.* **2010**, *20*, 7405−7415.
(32) Jayswal, A. S.; Chudasama, U. Synthesis and characterization of a novel metal phosphonate−zirconium(IV) hydroxy ethylidene diphosphonate and its application in separation of metal ions. *Asian J. Water Environ. Pollut.* **2008**, *6*, 97−101.
(33) Jayswal, A.; Chudasama, U. Synthesis and characterization of a novel metal phosphonate, zirconium(IV)-hydroxy ethylidene diphosphonate, and its application as an ion exchanger. *Turk. J. Chem.* **2008**, *32*, 63−74.
(34) Zhang, X. J.; Ma, T. Y.; Yuan, Z. Y. Titania−phosphonate hybrid porous materials: Preparation, photocatalytic activity and heavy metal ion adsorption. *J. Mater. Chem.* **2008**, *18*, 2003−2010.
(35) Holz, R. C.; Meister, G. E.; Horrocks, W. D. Spectroscopic characterization of a series of europium(III) amino phosphonate complexes in solution. *Inorg. Chem.* **1990**, *29*, 5183−5189.
(36) Ma, T. Y.; Yuan, Z. Y. Organic-additive-assisted synthesis of hierarchically meso-/microporous titanium phosphonates. *Eur. J. Inorg. Chem.* **2010**, 2941−2948.
(37) Zhu, Y. P.; Liu, Y. L.; Ren, T. Z.; Yuan, Z. Y. Hollow manganese phosphonate microspheres with hierarchical porosity for efficient adsorption and separation. *Nanoscale* **2014**, *6*, 6627−6636.
(38) Patel, P.; Chudasama, U. Synthesis and characterization of a novel hybrid cation exchange material and its application in metal ion separations. *Ion Exch. Lett.* **2011**, *4*, 7−15.
(39) Patel, P.; Chudasama, U. Application of a Novel Hybrid Cation Exchange Material in Metal Ion Separations. *Sep. Sci. Technol.* **2011**, *46*, 1346−1357.
(40) Shah, B.; Chudasama, U. Application of zirconium phosphonate—A novel hybrid material as an ion exchanger. *Desalin. Water Treat.* **2012**, *38*, 227−235.
(41) Thakkar, R.; Chudasama, U. Synthesis and characterization of zirconium titanium phosphate and its application in separation of metal ions. *J. Hazard. Mater.* **2009**, *172*, 129−137.
(42) Helfferich, F. *Ion Exchange*; McGraw-Hill: New York, 1962.
(43) Kunin, R. *Ion Exchange Resin*; Wiley: London, 1958.
(44) Maheria, K.; Chudasama, U. Kinetics, thermodynamics and sorption characteristics of an inorganic ion exchanger, titanium phosphate, towards first row transition metal ions. *Indian J. Chem.* **2007**, *46A*, 449−454.
(45) Bhaumik, A.; Inagaki, S. Mesoporous titanium phosphate molecular sieves with ion-exchange capacity. *J. Am. Chem. Soc.* **2001**, *123*, 691−696.
(46) Seip, C. T.; Granroth, G. E.; Miesel, M. W.; Talham, D. R. Langmuir−Blodgett films of known layered solids: Preparation and structural properties of octadecylphosphonate bilayers with divalent metals and characterization of a magnetic Langmuir Blodgett film. *J. Am. Chem. Soc.* **1997**, *119*, 7084−7094.
(47) Kurtoglu, A. E.; Atun, G. Determination of kinetics and equilibrium of Pb/Na exchange on clinoptilolite. *Sep. Purif. Technol.* **2006**, *50*, 62−70.
(48) Barrer, R. M. *Diffusion in and though Solids*; Cambridge University Press: New York, 1941.

(49) Barrer, R. M.; Fender, B. E. The diffusion and sorption of water in zeolites—II. Intrinsic and self-diffusion. *J. Phys. Chem. Solids* **1961**, *21*, 12−24.
(50) Barrer, R. M.; Bartholomew, R. F.; Rees, L. V. C. Ion exchange in porous crystals part I. Self- and exchange-diffusion of ions in chabazites. *J. Phys. Chem. Solids* **1963**, *24*, 51−62.
(51) Benyamin, K. Self-diffusion of sodium and cesium ions in hydrous titanium oxide. *Solid State Ionics* **1994**, *73*, 303−308.
(52) El-Batouti, M.; Zaghloul, A. A.; Hanna, M. T. A Kinetic Study of the Copper Exchange Reaction on a Sodium-Montmorillonite Clay Mineral in Acetonitrile and Dimethylformamide. *J. Colloid Interface Sci.* **1996**, *180*, 106−110.
(53) Low, K. S. Sorption of copper by dye-treated oil-palm fibres. *Bioresour. Technol.* **1993**, *44*, 109−112.
(54) Akpomie, G. K.; Ogbu, I. C.; Osunkunle, A. A.; Abuh, M. A.; Abonyi, M. N. Equilibrium Isotherm Studies on the Sorption of Pb(II) from Solution by Ehandiagu Clay. *J. Emerging Trends Eng. Appl. Sci.* **2012**, *3*, 354−358.
(55) Voudrias, E.; Fytianos, K.; Bozani, E. Sorption−desorption isotherms of dyes from aqueous solutions and wastewaters with different sorbent materials. *Global Nest* **2002**, *4*, 75−83.